Dephasing via stochastic absorption: A case study in Aharonov-Bohm oscill ations

Colin Benjamin* and A. M. Jayannavar†
Institute of Physics, Sachivalaya Marg, Bhubaneswar 751 005, Orissa, India
(Dated: February 1, 2008)

The Aharonov-Bohm ring has been the mainstay of mesoscopic physics research since its inception. In this paper we have dwelt on the problem of dephasing of AB oscillations using a phenomenological model based on stochastic absorption. To calculate the conductance in the presence of inelastic scattering we have used the method due to Brouwer and Beenakker. We have shown that conductance is symmetric under flux reversal and visibility of AB oscillations decay to zero as a function of the incoherence parameter thus signalling dephasing in the system. Some comments are made on the relative merits of stochastic absorption with respect to optical potential model, which have been used to mimic dephasing.

PACS numbers: 72.10.-d, 73.23.-b, 05.60.Gg, 85.35.Ds

Dephasing is defined as the process by which quantum mechanical interference is gradually destroyed[1,2]. Dephasing of electronic phase coherence may be caused by it's interaction with other quasi particles in the system. The notion of intrinsic decoherence and dephasing of a particle interacting with it's environment is being investigated intensively. For, a comparison between theory and experiment, it is necessary to know how dephasing affects the various quantum phenomena related to transport. In our present work we will be interested in modeling dephasing phenomenologically. The Aharonov-Bohm (AB) interferometer is one of the best examples for analyzing how quantum interference effects are affected by dephasing. In this interferometer the phase of the electrons passing through the arms is modulated by the magnetic flux. It is not unlike the Young's double slit experiment apart from the presence of the magnetic flux. In the Young's double slit interferometer as we know the intensity is given by $I = |\Psi|^2 = |\psi_1|^2 + |\psi_2|^2 + 2Re(\psi_1^* \psi_2 e^{i\phi})$, the part $2Re(\psi_1^* \psi_2 e^{i\phi})$ represents the interference term. Here ψ_1 and ψ_2 are the complex wave amplitudes across the upper and lower arms of the interferometer (this discussion is restricted to only two partial amplitudes for simplicity) and ϕ is phase difference between the two wave amplitudes. If there is no phase relationship between the waves then the intensity will be $I = |\psi_1|^2 + |\psi_2|^2$. Dephasing thus suppresses the interference terms. In other words dephasing, leads to the vanishing of the off-diagonal elements of the density matrix.

Aharonov-Bohm effect in mesoscopic rings manifests itself as a periodic behavior of conductance as a function of magnetic flux piercing the loop[1]. In an AB interferometer the electrons are treated quantum mechanically along the ring and they retain their phase memory across the entire sample and this gives rise to an operative definition of the phase coherence length L_ϕ or incoherence length. On increasing the temperature L_ϕ becomes less than the size of the ring and the phase coherence in the system gradually disappears and as a consequence the AB effect (the visibility of the AB oscillations) vanishes. Typically L_ϕ scales with temperature T in a power law form, i.e., $L_\phi = T^{-p}$ (p lies in the range 1 to 2).

There are different ways to model dephasing in such mesoscopic systems. A controlled way to introduce dephasing in the AB interferometer is to attach a voltage probe[3] to the sample as in inset of Fig. 1 (Buttiker's model). This voltage probe breaks the phase coherence by removing electrons from the phase coherent channel in the system and subsequently re-injecting them without any phase relationship. Another way to introduce dephasing, is to add a spatially uniform imaginary potential ($-iV_i$) (or optical potential) to the Hamiltonian[4], which removes particles from the phase coherent motion in the system. In this case absorbed particles are identified as a spectral weight lost in the inelastic channels and they are re-injected back into the sample. In the method due to Zohta and Ezawa[4] the total transmission is defined after re-injection as the sum of two contributions one due to the coherent part and the other due to the incoherent part, i.e., $T_{tot} = T_{coh} + T_{incoh}$. The incoherent part is calculated as $T_{incoh} = \frac{T_r}{T_l + T_r} A$, herein T_r and T_l are the probabilities for right and left transmission from the region of inelastic scattering and A is the absorbed part which is given by $A = 1 - T_{coh} - R_{coh}$. This model has been used by several other authors as well to simulate inelastic scattering. But, this model has a problem, in the presence of magnetic flux it is shown to violate the Onsager's two terminal symmetry relations[5], i.e., $T_{tot}(\Phi) \neq T_{tot}(-\Phi)$, where Φ is the magnetic flux, and hence is not suitable in modeling inelastic scattering whereas Buttiker's model preserves the Onsager's symmetry relations in the presence of magnetic flux. However, the Buttiker model suffers from a shortcoming, in that it describes only localized dephasing (at the point contact between system and third lead) instead of dephasing that occurs throughout the system in realistic situations.

Brouwer and Beenakker[6] have removed the shortcomings of both the above stated models by mapping the three probe Buttiker's method into a two terminal geometry, this is done by eliminating the transmission coefficients which explicitly depend on the third probe by means of unitarity of the S-matrix. They have considered a three terminal geometry in which one of the probes is

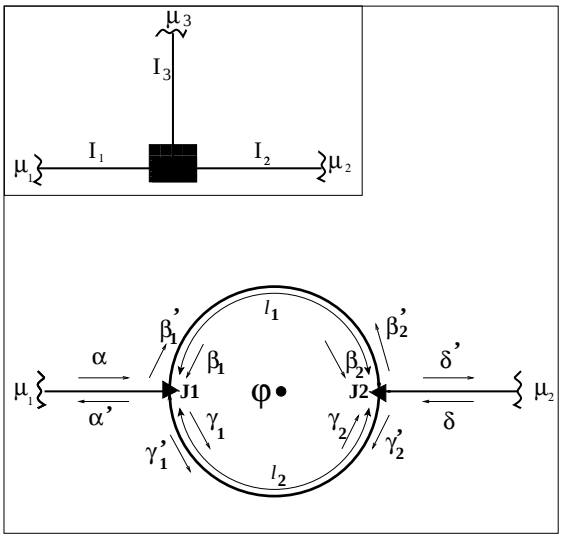

FIG. 1: Aharonov - Bohm ring geometry. Inset shows the three probe model.

used as a voltage probe in absence of magnetic flux (see inset of Fig. 1). A current $I = I_1 = -I_2$ flows from source to drain. In this model, a fictitious third lead connects the ring to a reservoir at chemical potential μ_3 in such a way that no current is drawn ($I_3 = 0$). The 3X3 S-matrix of the entire system can be written as-

$$S = \begin{pmatrix} r_{11} & t_{12} & t_{13} \\ t_{21} & r_{22} & t_{23} \\ t_{31} & t_{32} & r_{33} \end{pmatrix}$$

Application of the relations[3,6,7]- $I_p = \sum_q G_{pq}[\mu_p - \mu_q], p = 1, 2, 3$ and $G_{pq} = (2e^2/h)T_{pq}$

yields the (dimensionless) two probe conductance $G = \frac{h}{2e^2}\frac{I}{\mu_1 - \mu_2}$,

$$G = T_{21} + \frac{T_{23}T_{31}}{T_{31} + T_{32}} \tag{1}$$

and on elimination of the transmission coefficients which involve the voltage probe using the unitarity of the S - Matrix leads to[6]

$$G = T_{21} + \frac{(1 - R_{11} - T_{21})(1 - R_{22} - T_{21})}{1 - R_{11} - T_{21} + 1 - R_{22} - T_{12}}. \tag{2}$$

Now all the above coefficients are built from the 2X2 S matrix-

$$S' = \begin{pmatrix} r_{11} & t_{12} \\ t_{21} & r_{22} \end{pmatrix}$$

which represents the S Matrix of the absorbing system. The first term in Eq. 2 represents the conductance contribution from the phase coherent part. The second term accounts for electrons that are re-injected from the phase breaking reservoir, thereby ensuring particle conservation in the voltage probe model. For further calculation one can use the coefficients of the S' matrix of an absorbing system where absorption takes place uniformly.

There are different ways of introducing absorption in the system -(1) The well known imaginary potential (IP) model and (2)Stochastic absorption (SA). In the first case Hamiltonian becomes non-hermitian due to the presence of complex potential term $-iV_i$, which leads to absorption (non conservation of particle number). This model suffers from some spurious features[8,9]. In the scattering case, in the vicinity of the absorber, the particle experiences a mismatch in the potential (being complex) and therefore it tries to avoid this region by enhanced back reflection. Thus the IP model plays a dual role of an absorber as well as a reflector, i.e., absorption without reflection is not possible. Naively one expects the absorption to increase monotonically as a function of V_i. However, the observed behavior is non-monotonic. At first absorption increases and after exhibiting a maximum decreases to zero as $V_i \to \infty$. The absorber in this limit acts as a perfect reflector. During each scattering event an electron picks up an additional scattering phase shift due to V_i which along with multiple reflections leads to spurious scatterings (additional resonances)[8,9] in the system. As a result of the afore mentioned limitations there is need of a model wherein such spurious scatterings are absent and in the limit of large absorption does not correspond to a perfect reflector. Fortunately such a model exists, and this is the model of stochastic absorption[10]. This model does not suffer from the drawbacks of the IP model as we will show towards the end of our work.

The SA model is not new it has earlier been dealt with in the context of ID localization[10]. Stochastic absorption in the ring is inserted by the factor $e^{-\alpha l_1}$ (or $e^{-\alpha l_2}$) in the complex free propagator amplitudes, every time we traverse[7] the upper (or lower) arms of the ring (see Fig. 1). We have calculated the relevant transmission and reflection coefficients by using the S matrix method along with the quantum wave guide theory for a single channel case. In this model, average absorption per unit length is given by 2α. With this method we show that the calculated conductance (G) in Eq. 2 is symmetric under the flux reversal as required. The visibility of the AB oscillations rapidly decay as a function of α, indicating dephasing. Hence forth we refer to α as an incoherence parameter. Increasing α corresponds to increasing dephasing processes in the system or increase in temperature.

In Fig. 1, the length of the upper arm is l_1 and that of lower arm is l_2. The total circumference of the loop is $L = l_1 + l_2$. The loop is connected to two current leads. The couplers (triangles) in Fig. 1 which connects the leads and the loop are described by a scattering matrix S. The S matrix for the left coupler yields the amplitudes $O_1 = (\alpha', \beta_1', \gamma_1')$ emanating from the coupler in terms of the incident waves $I_1 = (\alpha, \beta_1, \gamma_1)$, and for the right coupler yields the amplitudes $O_2 = (\delta', \beta_2', \gamma_2')$ emanating from

the coupler in terms of the incident waves $I_2 = (\delta, \beta_2, \gamma_2)$. The S-matrix for either of the couplers[11] is given by-

$$S = \begin{pmatrix} -(a+b) & \sqrt{\epsilon} & \sqrt{\epsilon} \\ \sqrt{\epsilon} & a & b \\ \sqrt{\epsilon} & b & a \end{pmatrix}$$

with $a = \frac{1}{2}(\sqrt{(1-2\epsilon)} - 1)$ and $b = \frac{1}{2}(\sqrt{(1-2\epsilon)} + 1)$. ϵ plays the role of a coupling parameter. The maximum coupling between reservoir and loop is $\epsilon = \frac{1}{2}$, and for $\epsilon = 0$, the coupler completely disconnects the loop from the reservoir. As mentioned above incoherence is taken into account by introducing an attenuation constant per unit length as mentioned before.

The waves incident into the branches of the loop are related by the S Matrices for upper branch by-

$$\begin{pmatrix} \beta_1 \\ \beta_2 \end{pmatrix} = \begin{pmatrix} 0 & e^{ikl_1} e^{-\alpha l_1} e^{\frac{-i\theta l_1}{L}} \\ e^{ikl_1} e^{-\alpha l_1} e^{\frac{i\theta l_1}{L}} & 0 \end{pmatrix} \begin{pmatrix} \beta_1' \\ \beta_2' \end{pmatrix}$$

and for lower branch-

$$\begin{pmatrix} \gamma_1 \\ \gamma_2 \end{pmatrix} = \begin{pmatrix} 0 & e^{ikl_2} e^{-\alpha l_2} e^{\frac{i\theta l_2}{L}} \\ e^{ikl_2} e^{-\alpha l_2} e^{\frac{-i\theta l_2}{L}} & 0 \end{pmatrix} \begin{pmatrix} \gamma_1' \\ \gamma_2' \end{pmatrix}$$

These S matrices of course are not unitary $S(\alpha)S(\alpha)^\dagger \neq 1$ but they obey the relation $S(\alpha)S(-\alpha)^\dagger = 1$. The same relation is also obeyed by the S Matrix of the system in presence of imaginary potential. Here kl_1 and kl_2 are the phase increments of the wave function in absence of flux. $\frac{\theta l_1}{L}$ and $\frac{\theta l_2}{L}$ are the phase shifts due to flux in the upper and lower branches. Clearly, $\frac{\theta l_1}{L} + \frac{\theta l_2}{L} = \frac{2\pi\Phi}{\Phi_0}$, where Φ is the flux piercing the loop and Φ_0 is the flux quantum $\frac{hc}{e}$. The transmission and reflection coefficients in Eq. 2 are given as follows- $T_{21} = |\frac{\delta'}{\alpha}|^2$, $R_{11} = |\frac{\alpha'}{\alpha}|^2$, $R_{22} = |\frac{\delta'}{\delta}|^2$, $T_{12} = |\frac{\alpha'}{\delta}|^2$ wherein $\delta', \delta, \alpha', \alpha$ are as depicted in Fig. 1.

After calculating the required reflection and transmission coefficients we graphically represent our results in the following figures. Throughout the discussion the physical parameters we give are in dimensionless units. We see that the coherent transmission T_{21} is not symmetric under the flux reversal however proper re-injection of carriers by Eq. 2 for the total conductance G plotted in Fig. 2 shows that the Onsager's symmetry relations are restored, i.e., G is symmetric under flux reversal. In the inset of Fig. 2 we have plotted G versus flux for the same physical parameters except we have considered the weak coupling case ($\epsilon = 0.10$). G is symmetric in flux and features are sharp as expected because of lifetime broadening of the energy levels is small in this case compared to the case for which $\epsilon = 0.44$.

In Fig. 3 we plot visibility (V) as a function of incoherence parameter α. Visibility is of course defined as-

$$V = \frac{G_{max} - G_{min}}{G_{max} + G_{min}}. \quad (3)$$

The plot shows that with increase in the value of the parameter α the visibility exponentially falls off, reaching a point where it becomes zero corresponding to the disappearance of quantum interference effects. In the inset of Fig. 3 we have plotted the first few Fourier[13] harmonics a_i (wherein $i = 1$ to 4) of $G(\Phi)$ as a function of α. The harmonics exponentially fall off with increasing α with exponent increasing as we go from 1 to 4. The nth order harmonic corresponds to the contribution from electronic

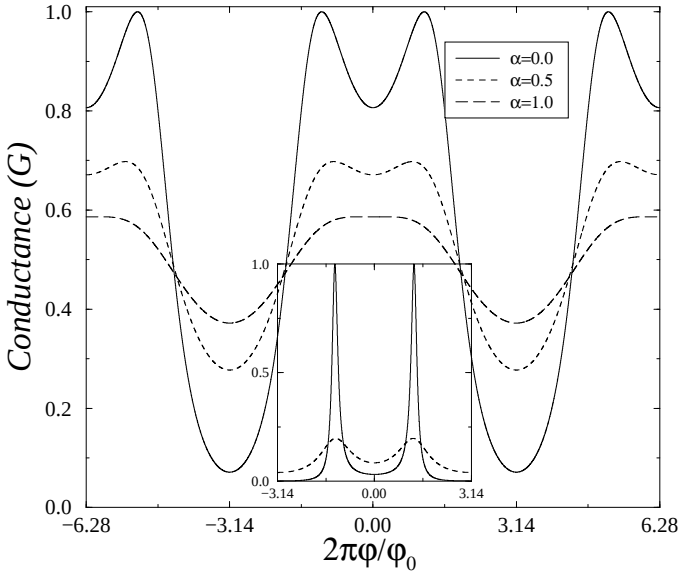

FIG. 2: Conductance (G)for lengths $l_1/l = 0.45$, $l_2/l = 0.55$ for coupling parameter $\epsilon = 0.44$ (waveguide coupling). Fermi wave-vector $kl = 5.0$. The inset shows the weak coupling case $\epsilon = 0.10$ for same physical parameters.

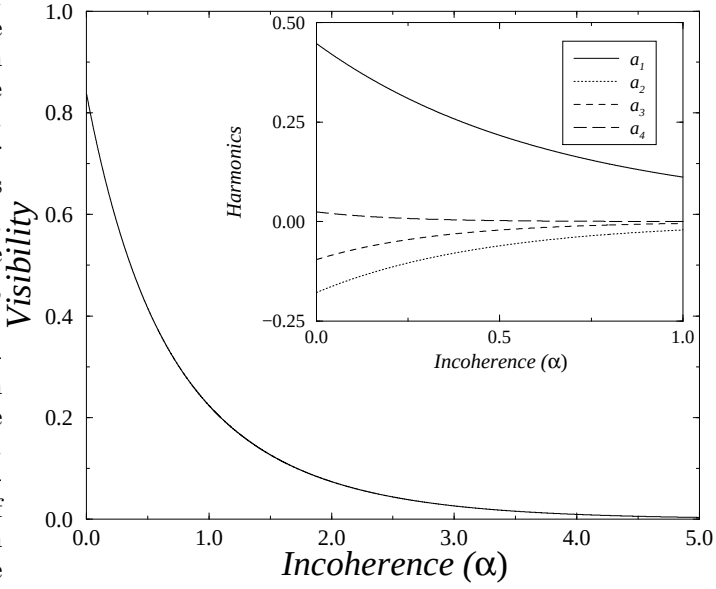

FIG. 3: Visibility for the same physical parameters as in figure 2, coupling parameter $\epsilon = 0.44$. In the inset the harmonics have been plotted for the same physical and coupling parameters.

paths which encircle the flux n times. The harmonics can sometimes show non monotonic behavior depending on the physical parameters, however, the visibility is a monotonic function of the incoherence parameter α.

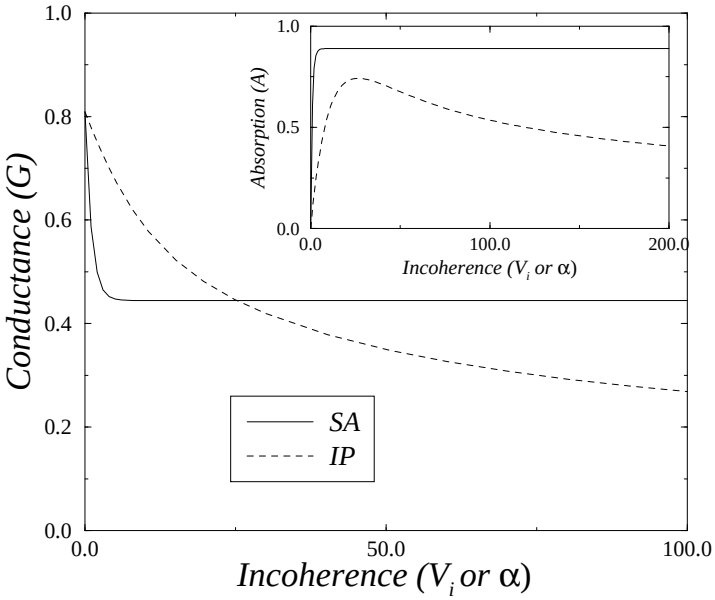

FIG. 4: Comparison of two models of dephasing. Herein the conductance (absorption in the inset) for the two cases SA and IP have been plotted. The parameters used are same as in Fig. 3.

Now for the comparison between the two models, i.e., IP and SA, in Fig. 4 we plot the total conductance (G) for both the cases. In the case of imaginary potential we see that the total conductance (G) continuously decreases and as $V_i \to \infty$, $G \to 0$ (this limit is not shown in the graph as it goes beyond the scale used), while in case of stochastic absorption as $\alpha \to \infty$, G goes to a constant value which depends on the Fermi-energy and other system parameters. Thus we see that the modeling of dephasing by SA is indeed justified as we want the AB oscillations to die out and not that the conductance itself should vanish, and this is where SA scores over the IP model. In the figure inset we have depicted the behavior of total absorption in the system A for both the cases for the same physical parameters. As $\alpha \to \infty$ there is a finite absorption in the system as the electron propagates in the medium in this limit whereas absorption in the imaginary potential model is non-monotonic and in the limit $V_i \to \infty$ absorption vanishes. This is due to the fact that in the IP model as $V_i \to \infty$ absorber acts as a perfect reflector, there is no absorption in the medium as the particles do not enter the medium (and hence $G = 0$) obviously which is an unrealistic situation for real systems.

In conclusion, we have shown that $G(\Phi)$ is symmetric under flux reversal in the presence of incoherent scattering represented by the incoherence parameter α. For this we have used the procedure of Brouwer and Beenakker in the presence of magnetic flux and simulated absorption (dephasing) using the method of stochastic absorption. We have used this method of SA to study the behaviors of the various quantum phenomena, e.g., transport across resonant tunneling systems, current magnification effect in mesoscopic rings,[12] delay and sojourn times[14] in mesoscopic systems in the presence of incoherence. These results will be published elsewhere.

Acknowledgments

One of us (AMJ) thanks Professor Markus Buttiker for his communication and his views on this problem.

* Electronic address: colin@iopb.res.in
† Electronic address: jayan@iopb.res.in

[1] Y.Imry, *Introduction to Mesoscopic Physics* (Oxford University Press, New York, 1997).
[2] Florian Marquardt, *An Introduction to the basics of dephasing* (http://iff.physik.unibas.ch/ florian/dephasing/dephasing.html).
[3] M. Buttiker, Phys. Rev. **B33**, 3020 (1986);IBM J. Res. Dev. **32**, 63 (1988).
[4] Y. Zohta and H. Ezawa , J. Appl. Phys. **72**, 3584 (1992).
[5] T. P. Pareek, S. K. Joshi and A. M. Jayannavar, Phys. Rev. **B57**, 8809 (1998).
[6] P. W. Brouwer and C. W. J. Beenakker , Phys. Rev. **B55**, 4695 (1997); P. W. Brouwer, Ph.D. thesis, Insttuut-Lorentz, University of Leiden, The Netherlands,1997.
[7] S. Datta, *Electron Transport in mesoscopic systems* (Cambridge University press, Cambridge, 1995).
[8] A. M. Jayannavar , Phys. Rev. **B49**, 14718 (1994); A. K. Gupta and A. M. Jayannavar,Phys. Rev. **B52**, 4156 (1995).
[9] A. Rubio and N. Kumar , Phys. Rev. **B47**, 2420 (1993).
[10] Sandeep K. Joshi, D. Sahoo and A. M. Jayannavar, Phys. Rev. **B62**, 880 (2000); P. Pradhan, preprint cond-mat/9807312.
[11] M. Buttiker, Y. Imry and M. Ya. Azbel, Phys. Rev. **A30**, 1982 (1984).
[12] A. M. Jayannavar and P. S. Deo, Phys. Rev. **B49**, 13685 (1994); T. P. Pareek, P. S. Deo and A. M. Jayannavar,Phys. Rev. **B52**, 14657 (1995); C. Benjamin and A. M. Jayannavar,Phys. Rev. **B64**, 233406 (2001).
[13] J. B. Xia, Phys. Rev. **B45**, 3593 (1992).
[14] S. Anantha Ramakrishna and N. Kumar, preprint cond-mat/0009269.